Published in final edited form as:
Neuron. 2014 May 21; 82(4): 836–847. doi:10.1016/j.neuron.2014.04.006.

The lipid kinase PIP5K1C regulates pain signaling and sensitization

Brittany D. Wright[1,3], **Lipin Loo**[3], **Sarah E. Street**[3], **Anqi Ma**[1,2], **Bonnie Taylor-Blake**[3], **Michael A. Stashko**[1,2], **Jian Jin**[1,2], **William P. Janzen**[1,2], **Stephen V. Frye**[1,2], and **Mark J. Zylka**[1,3,*]

[1]Division of Chemical Biology and Medicinal Chemistry, UNC Eshelman School of Pharmacy, The University of North Carolina at Chapel Hill, Chapel Hill, NC 27599, USA

[2]Center for Integrative Chemical Biology and Drug Discovery, The University of North Carolina at Chapel Hill, Chapel Hill, NC 27599, USA

[3]Department of Cell Biology and Physiology, UNC Neuroscience Center, The University of North Carolina at Chapel Hill, Chapel Hill, NC 27599, USA

SUMMARY

Numerous pain-producing (pronociceptive) receptors signal via phosphatidylinositol 4,5-bisphosphate (PIP_2) hydrolysis. However, it is currently unknown which lipid kinases generate PIP_2 in nociceptive dorsal root ganglia (DRG) neurons and if these kinases regulate pronociceptive receptor signaling. Here, we found that phosphatidylinositol 4-phosphate 5 kinase type 1C (PIP5K1C) is expressed at higher levels than any other PIP5K and, based on experiments with *Pip5k1c*$^{+/-}$ mice, generates at least half of all PIP_2 in DRG neurons. Additionally, *Pip5k1c* haploinsufficiency reduces pronociceptive receptor signaling and TRPV1 sensitization in DRG neurons as well as thermal and mechanical hypersensitivity in mouse models of chronic pain. We identified a novel small molecule inhibitor of PIP5K1C (UNC3230) in a high-throughput screen. UNC3230 lowered PIP_2 levels in DRG neurons and attenuated hypersensitivity when administered intrathecally or into the hindpaw. Our studies reveal that PIP5K1C regulates PIP_2- dependent nociceptive signaling and suggest that PIP5K1C is a novel therapeutic target for chronic pain.

INTRODUCTION

Tissue inflammation and nerve injury cause the release of a complex mix of chemicals that sensitize nociceptive dorsal root ganglia (DRG) neurons and contribute to chronic pain (Basbaum et al., 2009). These chemicals activate molecularly diverse pronociceptive receptors found on DRG neurons and their axon terminals. While these receptors represent attractive targets for analgesic drug development, efforts to block individual pronociceptive

*Corresponding author: zylka@med.unc.edu; 919-966-2540.

receptors have not yet produced effective treatments for chronic pain (Gold and Gebhart, 2010). This lack of efficacy could reflect the fact that multiple pronociceptive receptors are activated in the setting of chronic pain.

One approach to treat pain that bypasses this receptor diversity is to target points where different signaling pathways converge. Indeed, drugs that block signaling proteins that are several steps downstream from receptor activation, including protein kinase Cε (PKCε) and mitogen activated protein kinases (MAPKs), reduce nociceptive neuron sensitization, thermal hyperalgesia and mechanical allodynia in animal models (Aley et al., 2001; Aley et al., 2000; Cesare et al., 1999; Cheng and Ji, 2008; Dai et al., 2002; Ji et al., 2009; Ji et al., 2002). However, drugs that inhibit PKCε or MAPKs have shown modest-to-no efficacy in treating different pain conditions in humans (Anand et al., 2011; Cousins et al., 2013; Ostenfeld et al., 2013; Tong et al., 2011). This limited efficacy does not mean that PKCε or MAPK inhibitors cannot be used to treat pain, as drugs can show limited-to-no efficacy for a number of reasons, including the drugs may not engage their molecular target in humans or the drugs may lack efficacy in some pain conditions but not others.

Another convergence point, albeit one that has not been fully explored in the context of treating pain, is immediately downstream of multiple pronociceptive receptors. Many pronociceptive receptors, including Gq-coupled receptors, Gs-coupled receptors (via EPAC), and receptor tyrosine kinases, initiate signaling upon phospholipase C (PLC)-mediated hydrolysis of the lipid second messenger PIP_2 (Hucho et al., 2005). PIP_2 hydrolysis produces diacylglycerol (DAG) and inositol-1,4,5-trisphosphate (IP_3), which regulate nociceptive sensitization via multiple pathways, including PKCdependent modulation of ion channels like TRPV1, MAPK activation, and IP_3-mediated calcium influx (Falkenburger et al., 2010; Gamper and Shapiro, 2007; Gold and Gebhart, 2010; Rohacs et al., 2008; Tappe-Theodor et al., 2012). PIP_2 thus sits at a convergence point for diverse receptors and signaling pathways that promote and maintain nociceptive sensitization. In light of this information, we reasoned that it might be possible to reduce signaling through pronociceptive receptors and reduce pain sensitization by inhibiting the lipid kinase that generates the majority of all PIP_2 in DRG neurons.

Type 1 phosphatidylinositol 4-phosphate 5-kinases (*Pip5k1*s) generate PIP_2 by phosphorylating the 5 position on the inositol ring of phosphatidylinositol 4-phosphate [PI(4)P]. There are three mammalian *Pip5k1* genes (*Pip5k1a*, *Pip5k1b* and *Pip5k1c*) (Ishihara et al., 1998). Of these, *Pip5k1c* (also known as *Pip5k1γ*) is highly expressed in the brain (Wenk et al., 2001). PIP5K1C regulates receptor-mediated calcium signaling, actin cytoskeletal dynamics, endocytosis, and exocytosis (Di Paolo et al., 2004; Legate et al., 2012; Ling et al., 2002; Unoki et al., 2012; van den Bout and Divecha, 2009; Vasudevan et al., 2009; Volpicelli-Daley et al., 2010; Wang et al., 2007; Wang et al., 2004; Xu et al., 2010; Yu et al., 2011).

Previous studies examined the functions of *Pip5k1c* in the brain of knockout mice (Di Paolo et al., 2004; Rodriguez et al., 2012; Volpicelli-Daley et al., 2010; White et al., 2013). Homozygous (*Pip5k1*$c^{-/-}$) knockout mice have ~50% less PIP_2 in their brains and die within 24 hours of birth due to impaired mobility and an inability to feed (Di Paolo et al.,

2004; White et al., 2013). These data suggest a critical role for PIP5K1C in generating PIP_2 in neurons and in nervous system development. In contrast, heterozygous (*Pip5k1c*$^{+/-}$) mice are viable, reproduce normally, have normal levels of PIP_2 in the brain and showed no phenotypes in an extensive battery of tests, including multiple tests of neurological function (Di Paolo et al., 2004; White et al., 2013). The only phenotype observed thus far in *Pip5k1c*$^{+/-}$ mice is high-frequency (>20 kHz) hearing loss (Rodriguez et al., 2012), a phenotype ascribed to *Pip5k1c* haploinsufficiency in non-sensory cells of the auditory system.

When we initiated our studies, it was unknown which enzymes generated PIP_2 in nociceptive DRG neurons or if these enzymes regulated nociception. Here, we report that PIP5K1C is expressed in nearly all DRG neurons, generates at least half of all PIP_2 in the DRG and regulates nociceptive sensitization in response to diverse stimuli that cause pain. Our studies are the first to validate PIP5K1C as an analgesic drug target and identify a PIP5K1C inhibitor that attenuates pain in animal models.

RESULTS

PIP5K1C generates at least half of all PIP_2 in DRG neurons

To determine which *Pip5k1*s were expressed in the DRG, we performed *in situ* hybridization with probes for the three known mammalian *Pip5k1* genes. We found that *Pip5k1c* was expressed at higher levels in adult mouse DRG than the two other *Pip5k1* genes and was expressed in nearly all DRG neurons (Figure 1A–1C). PIP5K1C is also present in the brain at higher levels than PIP5K1A and PIP5K1B (Akiba et al., 2002; Wenk et al., 2001). Consistent with widespread expression in all DRG neurons, based on *in situ* hybridization, *Pip5k1c* was expressed in virtually all peptidergic (96.7%; n=220 counted) and nonpeptidergic (96.1%; n=210 counted) nociceptive neurons, marked by Calcitonin gene-related peptide-alpha (*Cgrp*) and Prostatic acid phosphatase (*Pap*), respectively (Figure 1D and 1E) (McCoy et al., 2013; Zylka et al., 2008). Using a recently developed antibody (Hara et al., 2013), we found that PIP5K1C was present on the plasma membrane and in the cytoplasm of most DRG neurons (Figure S1A–C). PIP5K1C was highly colocalized with PAP (98.1%; n=2,672 counted), CGRP (97.5%; n=2,094 counted), and TRPV1 (92.2%; n=1,915 counted), markers of nociceptive neurons (Figure S1D-L). Moreover, *PIP5K1C* was expressed in human DRG at levels comparable to *CGRP* (Intensity values of 311 and 346, respectively, from Affymetrix GeneChip experiments).

We then quantified PIP5K1C protein and PIP_2 levels in the DRG of wild-type (WT; *Pip5k1c*$^{+/+}$), *Pip5k1c*$^{+/-}$, and *Pip5k1c*$^{-/-}$ embryonic (E17.5–E18.5) mice. We found that PIP5K1C protein and PIP_2 levels were reduced (by ~50%) in the DRG of *Pip5k1c*$^{+/-}$ embryonic mice (Figure 1F–1H). No PIP5K1C protein was detectable in DRG from *Pip5k1c*$^{-/-}$ embryonic mice, confirming complete gene knockout and that both antibodies used in our study specifically recognized PIP5K1C (Figure 1F–1G). In addition, PIP_2 was reduced by ~70% in DRG from *Pip5k1c*$^{-/-}$ embryonic mice (Figure 1H).

Unlike *Pip5k1*$^{-/-}$ mice which die at birth, *Pip5k1c*$^{+/-}$ mice live into adulthood and reproduce normally (Di Paolo et al., 2004). Therefore, we quantified PIP5K1C protein and

PIP_2 levels in the DRG from *Pip5k1c*$^{+/-}$ adult mice and WT littermate controls. PIP5K1C protein was reduced by ~40% and PIP_2 levels were reduced by ~50% in the DRG of *Pip5k1c*$^{+/-}$ mice (Figure 1I–1K). In contrast, PIP_2 was not reduced in spinal cord or brain from adult *Pip5k1c*$^{+/-}$ mice (Figure 1K). Likewise, using a different quantification method, PIP_2 was not reduced in the brain of embryonic *Pip5k1c*$^{+/-}$ mice (Di Paolo et al., 2004; Volpicelli-Daley et al., 2010). In addition, we used immunofluorescence staining to examine PIP_2 levels at the membrane of cultured DRG neurons taken from adult mice. Quantification of the average perimeter (membrane) staining intensity in confocal images revealed that membrane PIP_2 levels were reduced by ~50% in small-to-medium diameter (≤ 27 μm) neurons of *Pip5k1c*$^{+/-}$ mice compared to WT controls (Figure 1L and 1M). Taken together, our data indicate that PIP5K1C generates at least half of all PIP_2 in the DRG, including in small-to-medium diameter, presumably nociceptive, DRG neurons. Moreover, our data indicate that PIP_2 is reduced in DRG of *Pip5k1c*$^{+/-}$ adult mice, but is not reduced in other regions of the nervous system that process pain and somatosensory stimuli, including spinal cord and brain.

Pip5k1c haploinsufficiency attenuates pronociceptive receptor signaling

Diverse molecules cause pain by activating pronociceptive G protein-coupled receptors (GPCRs) in DRG neurons. Since PIP_2 levels in the membrane were reduced by ~50% in DRG neurons, we hypothesized that pronociceptive GPCRs that couple to phospholipases and PIP_2 hydrolysis would signal less effectively in *Pip5k1c*$^{+/-}$ mice. To test this hypothesis we used the ratiometric calcium (Ca^{2+}) indicator dye Fura-2-AM to quantify lysophosphatidic acid (LPA) and 17-phenyl trinor prostaglandin E2 (17-PT PGE_2) evoked calcium responses in small-to-medium diameter DRG neurons. LPA evokes Ca^{2+} influx in small-to-medium diameter DRG neurons and, when injected intrathecally (i.t.), produces a chemically-induced form of neuropathic pain that is dependent on LPA1 receptor activation (Elmes et al., 2004; Inoue et al., 2004). 17-PT PGE_2 is a selective agonist for G_q-coupled prostanoid receptors, a class of receptors that are implicated in pain hypersensitivity following inflammation (Kassuya et al., 2007; Minami et al., 1994). Following stimulation with LPA- or 17-PT PGE_2, calcium responses (quantified as area under the curve; AUC) were blunted in *Pip5k1c*$^{+/-}$ neurons compared to WT controls (Figure 2A–2D). Importantly, these signaling deficits could be restored to WT levels by delivering excess PIP_2 to *Pip5k1c*$^{+/-}$ neurons just prior to imaging (Figure 2A–2D). These data suggest that the signaling deficits observed in *Pip5k1c*$^{+/-}$ neurons were the result of reduced PIP_2 levels and were not due to poor cell health or PIP_2- independent signaling deficits. Moreover, KCl-evoked Ca^{2+} responses, which reflect activation of voltage-gated calcium channels, were not altered (Figure 2A, data not shown). The percentage of neurons responding to either ligand (LPA responders: mean 22.2 ± 2.9% for WT and 24.1 ± 3.7% for *Pip5k1c*$^{+/-}$; 17-PT PGE_2 responders: 6.0 ± 1.2% for WT and 4.7 ± 1.1% for *Pip5k1c*$^{+/-}$) and the average diameter of responding neurons was not significantly different between WT and *Pip5k1c*$^{+/-}$ cultures (data not shown). We also found that delivering excess PIP_2 to WT neurons did not elevate LPAor 17-PT PGE_2-evoked calcium responses beyond control levels, suggesting that PIP_2 levels are already saturated in WT neurons under our culture conditions. Collectively, our data reveal that PIP5K1C regulates signaling downstream from two pronociceptive receptors, one associated with neuropathic pain and the other with inflammatory pain.

Moreover, rescue experiments revealed that *Pip5k1c* regulates calcium signaling in DRG neurons via a PIP_2-dependent mechanism, placing PIP5K1C upstream of multiple signaling pathways implicated in pain sensitization (Figure 2E).

Pip5k1c haploinsufficiency reduces ligand-induced nocifensive behaviors

LPA and 17-PT PGE_2 induce GPCR-mediated nociceptive responses when injected into the hindpaw (Kassuya et al., 2007; Renback et al., 1999; Renback et al., 2000). To determine if these compounds signal less effectively in *Pip5k1c*$^{+/-}$ mice, we injected LPA (4.1 μg) or 17-PT PGE_2 (1.2 μg) into one hindpaw then monitored the duration of licking for 5 minutes. We found that *Pip5k1c*$^{+/-}$ mice spent less time licking their ligand-injected hindpaws when compared to WT littermates (Figure 2F). Reduced licking was not due to motor impairment, as there were no significant differences between WT and *Pip5k1c*$^{+/-}$ mice in the rotarod assay and gait was not impaired (stride or stance; Figure S2A–S2C). Moreover, acute responses to innocuous mechanical touch were not impaired in *Pip5k1c*$^{+/-}$ mice (Figure S2D).

There was also no loss of nociceptive neurons or terminals in spinal cord of *Pip5k1c*$^{+/-}$ mice (determined by immunostaining for CGRP and IB4-binding, markers of nociceptive neurons; Figure S3A-3J). And, excitatory synaptic transmission between sensory neurons and spinal dorsal horn neurons was not impaired in *Pip5k1c*$^{+/-}$ mice, assessed by measuring excitatory field potential (fEPSP) amplitude in spinal cord slices after stimulating the dorsal root with a suction electrode (Street et al., 2011). Specifically, we found no significant differences between genotypes in fEPSP amplitude at different stimulus strengths (Figure S3K), following synaptic depletion (Figure S3L and S3M) or during synaptic recovery (Figure S3N). These data also ruled out the possibility that synaptic transmission or synaptic vesicle trafficking was impaired in *Pip5k1c*$^{+/-}$ mice. Instead, our data suggest that reduced nocifensive licking in *Pip5k1c*$^{+/-}$ reflects reduced pronociceptive receptor activation *in vivo*.

Pip5k1c haploinsufficiency attenuates TRPV1 activation and sensitization

PIP_2 levels also affect the activity and sensitization of the capsaicin and noxious heat receptor TRPV1 (Lukacs et al., 2007; Rohacs et al., 2008). To determine if *Pip5k1c* haploinsufficiency affected TRPV1 activation, we stimulated cultured DRG neurons from WT and *Pip5k1c*$^{+/-}$ mice with a high concentration of capsaicin (1 μM) then monitored calcium responses. We found that capsaicin-evoked calcium responses were blunted in DRG neurons from *Pip5k1c*$^{+/-}$ mice (Figure 3A) and that addition of exogenous PIP_2 to *Pip5k1c*$^{+/-}$ neurons restored capsaicin-evoked calcium responses to WT levels (Figure 3A and 3B). These data are consistent with the literature showing that PIP_2 is required for full activity when TRPV1 is activated with a high concentration of capsaicin (Lukacs et al., 2007; Rohacs et al., 2008). To evaluate TRPV1 sensitization by a GPCR agonist, we stimulated DRG neurons with a submaximal capsaicin concentration (100 nM; to limit the effects of Ca^{2+}-induced desensitization), applied the GPCR agonist LPA (1 μM), and then stimulated with capsaicin again to assess TRPV1 activity. We found that LPA sensitized TRPV1 activity in neurons cultured from WT mice (AUC value increased from 6.3 ± 1.5 to 8.9 ± 1.5; unpaired t-test, $p<0.05$) (Figure 3C). In contrast, LPA failed to sensitize TRPV1 in

neurons cultured from *Pip5k1c*$^{+/-}$ mice (AUC value decreased from 8.8 ± 2.0 to 3.6 ± 0.7; suggesting TRPV1 was desensitized) (Figure 3C). This likely reflected normal desensitization of TRPV1 caused by repeated capsaicin pulses (Loo et al., 2012). Consistent with this possibility, we found that repeated application of capsaicin (without adding LPA) caused desensitization of TRPV1 (data not shown). There was no significant difference in AUC values between WT and *Pip5k1c*$^{+/-}$ neurons following the first application of this low (100 nM) dose of capsaicin, consistent with previous literature showing that TRPV1 activity is less affected by changes in PIP_2 levels at low capsaicin concentrations (Lukacs et al., 2007; Rohacs et al., 2008).

Next, we evaluated how *Pip5k1c* haploinsufficiency affected TRPV1-mediated nociception *in vivo*. Injection of capsaicin (intraplantar) produced mechanical allodynia in WT mice but not thermal hyperalgesia (Figure 3D, data not shown), consistent with a previous study (Gilchrist et al., 1996). However, capsaicin-induced mechanical allodynia was significantly blunted in *Pip5k1c*$^{+/-}$ mice (Figure 3D). *Pip5k1c*$^{+/-}$ mice also exhibited increased withdrawal latencies at 45°C, 50°C, and 55°C relative to WT mice in the restrained hot plate assay (Figure 3E). Taken together, these data suggest that *Pip5k1c* is required for appropriate activation and sensitization of TRPV1 and for normal responsiveness to noxious heat.

Pip5k1c haploinsufficiency impairs thermal and mechanical sensitization in models of chronic pain

Pronociceptive receptor activation can sensitize animals to noxious thermal and mechanical stimuli. Since pronociceptive receptors signaled less effectively *in vitro* and *in vivo*, we hypothesized that thermal and mechanical sensitization might be blunted in *Pip5k1c*$^{+/-}$ mice following inflammation or injury. Indeed, thermal hyperalgesia and mechanical allodynia were enduringly attenuated in *Pip5k1c*$^{+/-}$ mice in models of chemically induced neuropathic pain (i.t. injection of 1 nmol LPA), neuropathic pain caused by spared-nerve ligation and inflammatory pain following an intraplantar injection of complete Freund's adjuvant (CFA) (Figure 4A–4F). There were no significant differences in the contralateral (non-inflamed/non-injured) paw between WT and *Pip5k1c*$^{+/-}$ mice, and there were no significant differences in either paw at baseline (prior to LPA injection, nerve injury, or inflammation). Taken together, these data suggest that *Pip5k1c* regulates nociceptive sensitization in three different models of chronic pain, with initiating events at three different anatomical locations (intrathecal, peripheral nerves and hindpaw).

Identification of a small molecule PIP5K1C inhibitor that reduces membrane PIP_2 levels and reduces pronociceptive receptor signaling

At the time we began our research, there were no small molecule inhibitors of PIP5K1C or any other lipid kinase that directly generates PIP_2. Since small molecule inhibitors can provide a complimentary method to validate targets when compared to genetic methods and can establish target tractability for drug discovery efforts (Weiss et al., 2007), we set out to identify a selective small molecule inhibitor of PIP5K1C. Accordingly, we developed a high-throughput microfluidic mobility shift assay that separates fluorescein conjugated PI(4)P (substrate) from fluorescein conjugated PIP_2 (product) (Figure 5A and 5B). We used

this assay to screen a kinase-focused library (~5,000 compounds) for inhibitors of recombinant human PIP5K1C (data not shown, assay development and screen will be described in a subsequent paper. Human and mouse PIP5K1C are 96% identical at the amino acid level within the kinase domain and 92% identical across the entire protein). From this screen, we identified UNC3230 [5- (cyclohexanecarboxamido)-2-(phenylamino)thiazole-4-carboxamide] which had an IC_{50} of ~41 nM using the microfluidic mobility shift assay (Figure 5C). To assess selectivity, we screened UNC3230 against 148 kinases (see Experimental Procedures), covering all major branches of the kinome (Figure 5D). Remarkably, UNC3230 inhibited (ProfilerPro assays) or competitively interacted (DiscoveRX binding assays) with only five other kinases at our relatively high (10 μM) screening concentration (using 10% activity/binding remaining relative to control as the cutoff for each kinase group, except lipid kinases, where a more stringent 35% of control cutoff was used) (Figure 5D, Table 1). Notably, UNC3230 did not interact with PIP5K1A at 10 μM, a PIP5K family member that is highly similar (69% amino acid identity across the entire protein and 82% identity within the kinase catalytic domain) to PIP5K1C. And, based on dose-responses with the five kinases that were inhibited by UNC3230 at the 10 μM screening concentration, UNC3230 showed selectivity (K_d<0.2 μM; using competitive binding assays) for PIP5K1C and PIP4K2C (Phosphatidylinositol-5-phosphate 4-kinase, type II, gamma) (Figure 5E–5G). PIP5K1C and PIP4K2C directly generate PIP_2, albeit using different substrates; PI(4)P versus PI(5)P, respectively (Figure S4). UNC3230 represents the first reported inhibitor for these lipid kinases. Moreover, UNC3230 did not inhibit any of the other lipid kinases that regulate phosphoinositide levels, including phosphatidylinositol-4,5-bisphosphate 3-kinases (PIK3s, also known as PI3Ks) (Table 1, Figure S4). Note, PIP4K2C should not be confused with phosphatidylinositol 4-kinases (PI4Ks). PI4Ks generate PI(4)P from phosphatidylinositol and can be inhibited by wortmannin and phenylarsine oxide (PAO; Figure S4) (Sorensen et al., 1998).

Inhibition of PIP5K1C and/or PIP4K2C would be predicted to reduce PIP_2 levels, so we assessed how UNC3230 affected PIP_2 levels in DRG neurons by using the PIP_2- specific antibody. We found that membrane PIP_2 levels were significantly reduced by ~45% in DRG neurons treated with 100 nM UNC3230 (~2-fold above the IC_{50}) relative to vehicle controls (Figure 6A and 6B). PI(4)P is present at 10-fold higher concentration over PI(5)P in cells (Delage et al., 2013), making UNC3230 more likely to affect PIP_2 that is generated by PIP5K1C. In addition, we found that UNC3230 significantly reduced LPA-evoked calcium signaling in cultured DRG neurons relative to vehicle (Figure 6C and 6D). Collectively, our data indicate that UNC3230 represents a novel pharmacological probe that can be used to inhibit two lipid kinases that directly generate PIP_2. Moreover, our data suggest that UNC3230 blunts pronociceptive receptor signaling in DRG neurons in a manner that is analogous to *Pip5k1c* haploinsufficiency.

UNC3230 has antinociceptive effects when injected intrathecally or into an inflamed hindpaw

Next we monitored sensitivity in WT mice before and shortly after i.t. or intraperitoneal (i.p.) administration of UNC3230. We found that UNC3230 (2 nmol in 20% dimethylsulfoxide; DMSO) significantly increased noxious heat-evoked paw withdrawal

latency for two hours after i.t. injection (Figure 7A), indicating an antinociceptive effect. UNC3230 did not have an acute effect on mechanical sensitivity (Figure 7B) and did not exhibit antinociceptive activity when administered i.p. (Figure S5A). This lack of activity via the i.p. route could reflect different pharmacokinetic properties following systemic versus localized (i.t. or into hindpaw, see below) drug delivery. To evaluate dosedependence, we administered UNC3230 at 1, 2, and 3 nmol (i.t.). We did not observe antinociceptive activity at 1 nmol (in 20% DMSO) but observed antinociceptive activity at 2 nmol (in 20% DMSO) that was similar to 3 nmol (in 50% DMSO) (Figure 7A and data not shown). In contrast, an inactive analog that is structurally similar to UNC3230 (by addition of a methyl group to the primary amide) did not exhibit thermal antinociceptive activity (Figure S5B), suggesting the antinociceptive activity of UNC3230 reflects on-target engagement of PIP5K1C (Figure S5B). Lastly, UNC3230 (2 nmol, i.t.) did not affect performance in the rotarod assay (Figure S5C).

Given that UNC3230 blunted LPA-evoked signaling, and that LPA enduringly enhances thermal and mechanical sensitivity by activating LPA receptors over a brief three hour critical period (Ma et al., 2009), we next evaluated the extent to which UNC3230 could reduce LPA-evoked thermal and mechanical hypersensitivity. We administered UNC3230 (2 nmol; i.t.; versus vehicle) then one hour later co-injected 1 nmol LPA with UNC3230 (2 nmol, i.t.; versus vehicle). UNC3230 significantly blunted thermal hyperalgesia and mechanical allodynia compared to vehicle (Figure 7C and 7D). Next, we administered UNC3230 (2 nmol; i.t.) two hours before and two hours after injecting CFA into one hindpaw. We found that UNC3230 significantly blunted thermal hyperalgesia and mechanical allodynia in the CFA-inflamed hindpaw (relative to vehicle control) but did not affect thermal or mechanical sensitivity in the control (non-inflamed) hindpaw over a multiday time course (Figure 7E and 7F). To determine if UNC3230 had antinociceptive effects in animals with ongoing inflammation, we injected CFA into one hindpaw and then 48 h later injected UNC3230 (2 nmol; i.t.). UNC3230 significantly reduced existing CFA-induced thermal hyperalgesia (relative to vehicle control) (Figure 7G). UNC3230 did not affect existing mechanical allodynia when administered following CFA inflammation (data not shown). Additionally, peripheral administration of UNC3230 (8 nmol, into the CFA-inflamed hindpaw), reduced thermal hyperalgesia (Figure 7H). Taken together, these data suggest UNC3230 could be used to block the initiation of chronic pain, with effects on hypersensitivity that are similar in magnitude to *Pip5k1c* haploinsufficiency, and can reduce established pain hypersensitivity.

DISCUSSION

Our study provides the first evidence that PIP5K1C generates at least half of all PIP_2 in DRG neurons and is a critical regulator of nociceptive signaling and sensitization, including thermal and mechanical hypersensitivity in models of neuropathic and inflammatory pain, two common forms of chronic pain in humans. Our conclusions are supported by experiments with *Pip5k1c*$^{+/-}$ mice and with a small molecule inhibitor of PIP5K1C. *Pip5k1c* haploinsufficiency reduced PIP_2 levels in adult DRG by ~50% without affecting PIP_2 levels in adult brain or spinal cord (Figure 1K), making it unlikely that the phenotypes we observed were due to *Pip5k1c* haploinsufficiency in other regions of the nervous system.

Moreover, spinal delivery of UNC3230 recapitulated these antinociceptive phenotypes, suggesting that localized inhibition of PIP5K1C in adults (and not during development) is sufficient to reduce nociceptive sensitization.

With the possible exceptions of our intrathecal LPA experiment and intraplantar experiment (Figure 4A,B and Figure 7H), in no cases was sensitization restored to baseline levels in *Pip5k1c*$^{+/-}$ mice or following UNC3230 administration. This could reflect the fact that GPCR signaling was reduced, but not eliminated, in neurons from *Pip5k1c*$^{+/-}$ mice and following UNC3230 treatment. Moreover, there are likely additional enzymes in DRG that generate PIP_2 and contribute to pronociceptive receptor signaling. In support of this possibility, PIP_2 levels were not reduced to zero in DRG from *Pip5k1c*$^{-/-}$ (embryonic) mice (Figure 1H). There are additional signaling pathways and cellular mechanisms that contribute to nociceptive sensitization (Basbaum et al., 2009; Gold and Gebhart, 2010) and some of these mechanisms are likely to be independent of *Pip5k1c* and PIP_2.

Intrathecal injections target DRG and spinal cord (Luo et al., 2005). Our efforts to measure small and possibly localized changes in PIP_2 levels in DRG following intrathecal injection were unsuccessful (data not shown). Thus, we cannot rule out the possibility that UNC3230 affects nociceptive sensitization by inhibiting PIP5K1C in the DRG and/or spinal cord (PIP5K1C is expressed by spinal neurons but is not expressed by spinal microglial cells; Allen Brain Atlas and data not shown). However, given that UNC3230 had antinociceptive effects when injected intrathecally as well as peripherally into the hindpaw, our data suggests that central or peripheral inhibition of PIP5K1C, presumably in primary sensory neurons or their afferents, is sufficient to reduce nociceptive responses. Moreover, PIP_2 levels were reduced in DRG but not spinal cord or brain of *Pip5k1c*$^{+/-}$ mice, suggesting the antinociceptive phenotypes in *Pip5k1c*$^{+/-}$ mice were due to reduced activity of PIP5K1C in primary sensory neurons.

As for why PIP_2 levels were reduced in DRG of *Pip5k1c*$^{+/-}$ mice but not spinal cord or brain, we speculate this reflects a greater dependence on *Pip5k1c* in DRG relative to these other tissues. In support of this idea, PIP_2 levels were not reduced in the brain of *Pip5k1c*$^{+/-}$ mice (Figure 1K) (Volpicelli-Daley et al., 2010), but were reduced by 50% in the brain of embryonic *Pip5k1c*$^{-/-}$ mice (Volpicelli-Daley et al., 2010; Wang et al., 2007). Thus, PIP_2 levels in the central nervous system appear to be insensitive to *Pip5k1c* haploinsufficiency. Additionally, PIP_2 levels were not reduced in the brain of embryonic *Pip5k1a*, *Pip5k1b* double knockout mice, suggesting other enzymes besides *Pip5k1a*, *Pip5k1b*, or *Pip5k1c* generate PIP_2 in the nervous system (Volpicelli-Daley et al., 2010). This greater dependence on *Pip5k1c* in DRG makes this lipid kinase a particularly attractive target for analgesic drug development, as inhibition of PIP5K1C has the potential to lower PIP_2 levels in primary sensory neurons to a greater extent than in the brain.

PIP5K1C modulates pronociceptive receptor signaling via a PIP_2-dependent mechanism

PIP_2-dependence was supported by the fact that addition of PIP_2 rescued signaling deficits in *Pip5k1c*$^{+/-}$ neurons. Others similarly found that PIP_2 addition rescued histamine-evoked calcium responses in HeLa cells following *Pip5k1c* knockdown (Wang et al., 2004). And, ATP-evoked calcium release from purinergic receptors was significantly blunted in

Pip5k1c$^{+/-}$ lateral nonsensory cells (Rodriguez et al., 2012), further indicating that *Pip5k1c* regulates receptor signaling. Furthermore, our data reveals that *Pip5k1c* haploinsufficiency eliminates GPCR-mediated sensitization of TRPV1 (Figure 3C).

Pip5k1c regulates many additional processes downstream of PIP_2, including actin dynamics, synaptic vesicle release and NMDA-induced AMPA receptor endocytosis (Rusinova et al., 2013; Toth et al., 2012; Unoki et al., 2012; van den Bout and Divecha, 2009). We ruled out the possibility that neurotransmission was impaired between sensory neurons and spinal neurons in *Pip5k1c*$^{+/-}$ mice, making it unlikely that vesicle recycling deficits accounted for reduced behavioral sensitization. However, we cannot exclude the possibility that other mechanisms downstream of PIP_2 are impaired in *Pip5k1c*$^{+/-}$ mice. Future studies will be needed to assess the relative contribution of these downstream mechanisms to nociceptive deficits in *Pip5k1c*$^{+/-}$ mice.

PIP5K1C is a novel analgesic drug target

The antinociceptive phenotypes in *Pip5k1c*$^{+/-}$ mice motivated us to develop a high-throughput screen for PIP5K1C inhibitors. From this screen, we identified UNC3230, a compound that inhibited PIP5K1C in the nanomolar range and that reduced receptor signaling and nociceptive sensitization analogous to *Pip5k1c* haploinsufficiency. While we evaluated the specificity of UNC3230 relative to a large panel of kinases, we cannot exclude the possibility that UNC3230 inhibits kinases that were not available for testing, including additional kinases that generate PIP_2. Given that UNC3230 reduced PIP_2 levels in DRG and had antinociceptive activity *in vivo*, whereas an inactive close analog of UNC3230 did not have antinociceptive activity, these data suggest that UNC3230 has on-target biochemical effects. UNC3230 showed selectivity for PIP5K1C and PIP4K2C, two lipid kinases that directly generate PIP_2. The DiscoveRx Selectivity Profile score for UNC3230 was 0.12 (on a scale from 0 to 1.0) (Karaman et al., 2008). To put this value in context, of 38 kinase inhibitors (several of them FDA-approved) benchmarked in this assay at 3 μM (Karaman et al., 2008), a majority (n=22) were less selective than UNC3230.

Our genetic and pharmacological data validate PIP5K1C as a therapeutic target for chronic pain; however, further optimization of hits from our high-throughput screen is warranted. For example, UNC3230 has a narrow efficacy window and low solubility in appropriate vehicles that limited our ability to perform dose-responses *in vitro* and *in vivo*. These shortcomings may be overcome through subsequent medicinal chemistry optimization, particularly given that PIP5K1C inhibitors could provide an alternative to opioid and non-steroidal anti-inflammatory analgesics. Moreover, PIP5K1C inhibitors will likely have uses that extend beyond the nociceptive system, such as to study how transient PIP5K1C inhibition affects other processes linked to PIP5K1C.

There are a number of additional enzymes that could affect PIP_2 levels in DRG neurons, including lipid kinases other than PIP5K1C, phosphatases and lipid transporters. Our current study suggests these additional enzymes represent attractive targets for analgesic drug development. In support of this idea, a functional-genomics study in *Drosophila* identified phospholipid signaling and lipid kinases as key regulators of heat nociception (Neely et al., 2012). This study also found that *Pip5k1a*$^{-/-}$ mice (not *Pip5k1c*) displayed hypersensitivity

to noxious heat and capsaicin. However, given that *Pip5k1a* is expressed at much lower levels in DRG (Figure 1A) and does not contribute to PIP_2 levels in the central nervous system (Volpicelli-Daley et al., 2010), precisely how and where *Pip5k1a* regulates heat nociception in mice is unclear.

Human implications

Humans carrying heterozygous null mutations in *Pip5k1c* (i.e. *PIP5K1C*$^{+/-}$ humans) develop normally and appear healthy (Narkis et al., 2007). Since humans apparently can tolerate a life-long reduction in *PIP5K1C* gene dosage, drugs that transiently inhibit PIP5K1C have the potential to be well-tolerated—particularly in adults—the age group that suffers most from chronic pain. The high frequency hearing loss seen in *Pip5k1c*$^{+/-}$ mice is not likely to be an issue in humans because humans cannot hear above 20 kHz (Brant and Fozard, 1990). In contrast, *PIP5K1C*$^{-/-}$ humans develop lethal congenital contracture syndrome type 3, which is characterized by muscle atrophy, joint contractures and death within 24 hours of birth (Narkis et al., 2007). The human phenotype closely mimics the perinatal lethality observed in the *Pip5k1c*$^{-/-}$ mice (Di Paolo et al., 2004). It is currently unknown if *PIP5K1C*$^{+/-}$ humans have reduced pain responses, as we found with *Pip5k1c*$^{+/-}$ mice. Future studies with these human carriers have the potential to directly assess the importance of PIP5K1C in human pain perception.

Intriguingly, the individuals that carry the *PIP5K1C* mutation (*PIP5K1C*$^{+/-}$) are Bedouins and live in the Negev desert of Israel—an environment that is arid and subject to extreme temperatures. Like sickle-cell anemia, where heterozygotes (carriers) have a survival advantage in regions where malaria is endemic, mutations in PIP5K1C might provide a survival advantage in the desert, where somatosensory stimuli can be extreme.

EXPERIMENTAL PROCEDURES

Animals

All procedures involving vertebrate animals were approved by the Institutional Animal Care and Use Committee at the University of North Carolina at Chapel Hill. *Pip5k1c*$^{+/-}$ mice were provided by Pietro De Camilli at Yale University (also available from The Jackson Laboratory, #008515) (Di Paolo et al., 2004). All mice were backcrossed to C57BL/6 mice for at least 10 generations.

Immunostaining

Lumbar DRG and spinal cord were dissected from adult (6–8 week old) male mice and immunostained as previously described (McCoy et al., 2013; Zylka et al., 2008).

ELISA PIP_2 quantification

$PI(4,5)P_2$ mass ELISA was purchased from Echelon Biosciences (K-4500) and performed according to the manufacturer's instructions with the following alterations. Lumbar DRG (L3-L5, bilateral), lumbar spinal cord and cerebral cortex were dissected from adult male mice (6–8 weeks old) and all DRG were dissected from embryos (E17.5–18.5). All tissue was frozen immediately on dry ice. Tissue was homogenized and sonicated prior to lipid

extraction. DRG samples were diluted 1:40 and spinal cord and brain samples were diluted 1:200 prior to use in the ELISA assay. Bicinchoninic acid (BCA) protein determination assay (ThermoScientific, 23225) was completed for each sample following the manufacturer's instructions. Protein content for each sample was used for normalization.

Neuron culture and calcium imaging

All DRG were dissected from 3–8 week old male mice following decapitation and cultured as described (see Supplemental Experimental Procedures). Calcium imaging of dissociated neurons was completed as described previously using Fura 2- acetoxymethyl ester (2 μM; F1221, Invitrogen) (McCoy et al., 2013).

Behavioral assays

Pronociceptive ligands (4.1 μg LPA; 1.2 μg 17-PT PGE_2, in 0.9% saline) were injected into the left hindpaw and the amount of time spent licking was measured for 5 minutes. Thermal and mechanical sensitivity were monitored before and 30 minutes after capsaicin (2 μg) injection. Thermal sensitivity was measured using a Plantar Test apparatus (IITC) to heat each hindpaw and the latency for hindpaw removal was recorded. One measurement was taken for each hindpaw to determine the withdrawal latency in seconds. The radiant heat source intensity was calibrated so that the average withdrawal latency for WT mice was ~10 s. Cut off time was 20 s. Mechanical sensitivity was measured using an electronic von Frey apparatus (IITC) and a semi-flexible tip. Three measurements for each hindpaw were taken and averaged to determine the withdrawal threshold in grams. For the restrained hot plate test, animals were restrained by scruffing and the right hindpaw was placed on a metal surface of the indicated noxious temperature. The latency for the animal to withdrawal (lift, shake, or jump) its hindpaw was recorded. Inflammatory (CFA) and neuropathic (LPA and spared nerve injury) models of chronic pain were performed as described previously (Ma et al., 2009; Shields et al., 2003; Zylka et al., 2008). Intrathecal injections (5 μL) were performed in unanesthetized mice using the direct lumbar puncture method (Fairbanks, 2003). UNC3230 was prepared at a final concentration of 0.4 mM (2 nmol per 5 μL) in 20% DMSO or 0.6 mM in 50% DMSO for intrathecal injections. UNC3230 was prepared at a final concentration of 0.4 mM in 20% DMSO for intraplantar injections (20 μL per hindpaw; 8 nmol total). For intraperitoneal injections, 5 mM UNC3230 was prepared in 90% corn oil and 10% ethanol and administered at 20 mg/kg.

Small molecule inhibitor screen

N-terminal His_6-tagged full length (90 kDa) recombinant human PIP5K1C (Millipore 14-845) was incubated for 10 minutes in the presence or absence of small molecules in assay buffer (50 mM MOPS, 500 μM sodium cholate, 10 mM magnesium chloride, and 25 mM sodium chloride) in 384-well Nunc assay plates. Fluorescein conjugated substrate [PI(4)P; Cayman Chemical, 9000655] and ATP at the K_m concentration for PIP5K1C (15 μM) were added to the assay plates and incubated for 40 minutes. Reactions were stopped using 90 mM EDTA. Fluorescein conjugated PIP_2 and remaining PI(4)P were separated and quantified using the LabChip EZ Reader II microfluidic mobility shift assay (PerkinElmer). Validation of the assay was performed in duplicate using the library of pharmacologically

active compounds (LOPAC; Sigma), giving a r^2 value of 0.965. We used this assay to screen a focused kinase library (~5,000 compounds), which contained UNC3230.

Selectivity screening

Two different assays were used to assess selectivity. ProfilerPro (PerkinElmer) was used to assess selectivity of UNC3230 on 48 kinases. For the ProfilerPro assay, UNC3230 was added to reaction-ready (384-well) assay plates (PerkinElmer) containing each of the 48 kinases in duplicate and incubated for 15 minutes. Matching fluorescent substrates for each kinase (also provided in reaction-ready 384-well plates) and ATP at the K_m for each kinase were added then the plate was incubated for 90 minutes. Fluorescent substrates and products were separated and quantified using the LabChip EZ Reader II microfluidic mobility-shift assay (PerkinElmer). Data for this assay are reported as percent of control (product produced in the absence of UNC3230).

The DiscoveRx KINOMEscan competitive binding assay was used to quantitatively measure interactions between UNC3230 and 100 different kinases. Briefly, UNC3230 and each DNA-tagged kinase were added simultaneously to 384-well plates containing immobilized ligands for each of the 100 kinases tested. Plates were incubated for 1 hour and the amount of kinase bound to the immobilized ligand was quantified using qPCR and the associated DNA tag. Binding interactions were determined by the amount of kinase that bound to the immobilized ligand. Competitive interactions between the kinase and UNC3230 would prevent binding of the kinase to the immobilized ligand. Data for this assay are reported as percent of control (binding of a control compound to the kinase).

Supplementary Material

Refer to Web version on PubMed Central for supplementary material.

Acknowledgments

We thank Pietro De Camilli for providing *Pip5k1c* knockout mice and antibodies, Hiroyuki Sakagami for providing PIP5K1C antibody, Megumi Aita for performing *in situ* hybridization, Eric McCoy for independently replicating calcium imaging experiments, J. Walter Dutton for pilot behavioral experiments, Brendan Fitzpatrick for performing intrathecal injections and spared-nerve ligation surgeries, Kara Agster for performing rotarod assays and Gabriela Salazar for performing intrathecal injections and mouse colony management. In addition we thank Catherine Simpson, Chatura Jayakody, Emily Hull-Ryde, and Laurel Provencher (PerkinElmer) for help with HTS assay development and Dmitri Kireev for small molecule activity analysis. This work was supported by grants to M.J.Z. from NINDS (R01NS081127, R01NS067688). The BAC Core, Confocal Imaging Core and *in situ* Hybridization Core are funded by grants from NINDS (P30NS045892) and NICHD (P30HD03110).

References

Akiba Y, Suzuki R, Saito-Saino S, Owada Y, Sakagami H, Watanabe M, Kondo H. Localization of mRNAs for phosphatidylinositol phosphate kinases in the mouse brain during development. Brain Res Gene Expr Patterns. 2002; 1:123–133. [PubMed: 15018809]

Aley KO, Martin A, McMahon T, Mok J, Levine JD, Messing RO. Nociceptor sensitization by extracellular signal-regulated kinases. J Neurosci. 2001; 21:6933– 6939. [PubMed: 11517280]

Aley KO, Messing RO, Mochly-Rosen D, Levine JD. Chronic hypersensitivity for inflammatory nociceptor sensitization mediated by the epsilon isozyme of protein kinase C. J Neurosci. 2000; 20:4680–4685. [PubMed: 10844037]

Anand P, Shenoy R, Palmer JE, Baines AJ, Lai RY, Robertson J, Bird N, Ostenfeld T, Chizh BA. Clinical trial of the p38 MAP kinase inhibitor dilmapimod in neuropathic pain following nerve injury. Eur J Pain. 2011; 15:1040–1048. [PubMed: 21576029]

Basbaum AI, Bautista DM, Scherrer G, Julius D. Cellular and molecular mechanisms of pain. Cell. 2009; 139:267–284. [PubMed: 19837031]

Brant LJ, Fozard JL. Age changes in pure-tone hearing thresholds in a longitudinal study of normal human aging. J Acoust Soc Am. 1990; 88:813–820. [PubMed: 2212307]

Cesare P, Dekker LV, Sardini A, Parker PJ, McNaughton PA. Specific involvement of PKC-epsilon in sensitization of the neuronal response to painful heat. Neuron. 1999; 23:617–624. [PubMed: 10433272]

Cheng JK, Ji RR. Intracellular signaling in primary sensory neurons and persistent pain. Neurochem Res. 2008; 33:1970–1978. [PubMed: 18427980]

Cousins MJ, Pickthorn K, Huang S, Critchley L, Bell G. The safety and efficacy of KAI-1678- an inhibitor of epsilon protein kinase C (epsilonPKC)-versus lidocaine and placebo for the treatment of postherpetic neuralgia: a crossover study design. Pain Med. 2013; 14:533–540. [PubMed: 23438341]

Dai Y, Iwata K, Fukuoka T, Kondo E, Tokunaga A, Yamanaka H, Tachibana T, Liu Y, Noguchi K. Phosphorylation of extracellular signal-regulated kinase in primary afferent neurons by noxious stimuli and its involvement in peripheral sensitization. J Neurosci. 2002; 22:7737–7745. [PubMed: 12196597]

Delage E, Puyaubert J, Zachowski A, Ruelland E. Signal transduction pathways involving phosphatidylinositol 4-phosphate and phosphatidylinositol 4,5- bisphosphate: convergences and divergences among eukaryotic kingdoms. Prog Lipid Res. 2013; 52:1–14. [PubMed: 22981911]

Di Paolo G, Moskowitz HS, Gipson K, Wenk MR, Voronov S, Obayashi M, Flavell R, Fitzsimonds RM, Ryan TA, De Camilli P. Impaired PtdIns(4,5)P2 synthesis in nerve terminals produces defects in synaptic vesicle trafficking. Nature. 2004; 431:415–422. [PubMed: 15386003]

Elmes SJ, Millns PJ, Smart D, Kendall DA, Chapman V. Evidence for biological effects of exogenous LPA on rat primary afferent and spinal cord neurons. Brain Res. 2004; 1022:205–213. [PubMed: 15353230]

Fairbanks CA. Spinal delivery of analgesics in experimental models of pain and analgesia. Adv Drug Deliv Rev. 2003; 55:1007–1041. [PubMed: 12935942]

Falkenburger BH, Jensen JB, Dickson EJ, Suh BC, Hille B. Phosphoinositides: lipid regulators of membrane proteins. J Physiol. 2010; 588:3179–3185. [PubMed: 20519312]

Gamper N, Shapiro MS. Regulation of ion transport proteins by membrane phosphoinositides. Nat Rev Neurosci. 2007; 8:921–934. [PubMed: 17971783]

Gilchrist HD, Allard BL, Simone DA. Enhanced withdrawal responses to heat and mechanical stimuli following intraplantar injection of capsaicin in rats. Pain. 1996; 67:179–188. [PubMed: 8895246]

Gold MS, Gebhart GF. Nociceptor sensitization in pain pathogenesis. Nat Med. 2010; 16:1248–1257. [PubMed: 20948530]

Hara Y, Fukaya M, Tamaki H, Sakagami H. Type I phosphatidylinositol 4-phosphate 5-kinase gamma is required for neuronal migration in the mouse developing cerebral cortex. Eur J Neurosci. 2013; 38:2659–2671. [PubMed: 23802628]

Hucho TB, Dina OA, Levine JD. Epac mediates a cAMP-to-PKC signaling in inflammatory pain: an isolectin B4(+) neuron-specific mechanism. J Neurosci. 2005; 25:6119–6126. [PubMed: 15987941]

Inoue M, Rashid MH, Fujita R, Contos JJ, Chun J, Ueda H. Initiation of neuropathic pain requires lysophosphatidic acid receptor signaling. Nat Med. 2004; 10:712–718. [PubMed: 15195086]

Ishihara H, Shibasaki Y, Kizuki N, Wada T, Yazaki Y, Asano T, Oka Y. Type I phosphatidylinositol-4-phosphate 5-kinases. Cloning of the third isoform and deletion/substitution analysis of members of this novel lipid kinase family. J Biol Chem. 1998; 273:8741–8748. [PubMed: 9535851]

Ji RR, Gereau RWt, Malcangio M, Strichartz GR. MAP kinase and pain. Brain Res Rev. 2009; 60:135–148. [PubMed: 19150373]

Ji RR, Samad TA, Jin SX, Schmoll R, Woolf CJ. p38 MAPK activation by NGF in primary sensory neurons after inflammation increases TRPV1 levels and maintains heat hyperalgesia. Neuron. 2002; 36:57–68. [PubMed: 12367506]

Karaman MW, Herrgard S, Treiber DK, Gallant P, Atteridge CE, Campbell BT, Chan KW, Ciceri P, Davis MI, Edeen PT, et al. A quantitative analysis of kinase inhibitor selectivity. Nat Biotechnol. 2008; 26:127–132. [PubMed: 18183025]

Kassuya CA, Ferreira J, Claudino RF, Calixto JB. Intraplantar PGE2 causes nociceptive behaviour and mechanical allodynia: the role of prostanoid E receptors and protein kinases. Br J Pharmacol. 2007; 150:727–737. [PubMed: 17310141]

Legate KR, Montag D, Bottcher RT, Takahashi S, Fassler R. Comparative phenotypic analysis of the two major splice isoforms of phosphatidylinositol phosphate kinase type Igamma in vivo. J Cell Sci. 2012; 125:5636–5646. [PubMed: 22976293]

Ling K, Doughman RL, Firestone AJ, Bunce MW, Anderson RA. Type I gamma phosphatidylinositol phosphate kinase targets and regulates focal adhesions. Nature. 2002; 420:89–93. [PubMed: 12422220]

Loo L, Shepherd AJ, Mickle AD, Lorca RA, Shutov LP, Usachev YM, Mohapatra DP. The C-type natriuretic peptide induces thermal hyperalgesia through a noncanonical Gbetagamma-dependent modulation of TRPV1 channel. J Neurosci. 2012; 32:11942–11955. [PubMed: 22933780]

Lukacs V, Thyagarajan B, Varnai P, Balla A, Balla T, Rohacs T. Dual regulation of TRPV1 by phosphoinositides. J Neurosci. 2007; 27:7070–7080. [PubMed: 17596456]

Luo MC, Zhang DQ, Ma SW, Huang YY, Shuster SJ, Porreca F, Lai J. An efficient intrathecal delivery of small interfering RNA to the spinal cord and peripheral neurons. Mol Pain. 2005; 1:29. [PubMed: 16191203]

Ma L, Matsumoto M, Xie W, Inoue M, Ueda H. Evidence for lysophosphatidic acid 1 receptor signaling in the early phase of neuropathic pain mechanisms in experiments using Ki-16425, a lysophosphatidic acid 1 receptor antagonist. J Neurochem. 2009; 109:603–610. [PubMed: 19222705]

McCoy ES, Taylor-Blake B, Street SE, Pribisko AL, Zheng J, Zylka MJ. Peptidergic CGRPalpha primary sensory neurons encode heat and itch and tonically suppress sensitivity to cold. Neuron. 2013; 78:138–151. [PubMed: 23523592]

Minami T, Nishihara I, Uda R, Ito S, Hyodo M, Hayaishi O. Characterization of EP-receptor subtypes involved in allodynia and hyperalgesia induced by intrathecal administration of prostaglandin E2 to mice. Br J Pharmacol. 1994; 112:735–740. [PubMed: 7921597]

Narkis G, Ofir R, Landau D, Manor E, Volokita M, Hershkowitz R, Elbedour K, Birk OS. Lethal contractural syndrome type 3 (LCCS3) is caused by a mutation in PIP5K1C, which encodes PIPKI gamma of the phophatidylinsitol pathway. Am J Hum Genet. 2007; 81:530–539. [PubMed: 17701898]

Neely GG, Rao S, Costigan M, Mair N, Racz I, Milinkeviciute G, Meixner A, Nayanala S, Griffin RS, Belfer I, et al. Construction of a global pain systems network highlights phospholipid signaling as a regulator of heat nociception. PLoS Genet. 2012; 8:e1003071. [PubMed: 23236288]

Ostenfeld T, Krishen A, Lai RY, Bullman J, Baines AJ, Green J, Anand P, Kelly M. Analgesic efficacy and safety of the novel p38 MAP kinase inhibitor, losmapimod, in patients with neuropathic pain following peripheral nerve injury: a double-blind, placebo-controlled study. Eur J Pain. 2013; 17:844–857. [PubMed: 23239139]

Renback K, Inoue M, Ueda H. Lysophosphatidic acid-induced, pertussis toxin-sensitive nociception through a substance P release from peripheral nerve endings in mice. Neurosci Lett. 1999; 270:59–61. [PubMed: 10454146]

Renback K, Inoue M, Yoshida A, Nyberg F, Ueda H. Vzg- 1/lysophosphatidic acid-receptor involved in peripheral pain transmission. Brain Res Mol Brain Res. 2000; 75:350–354. [PubMed: 10686359]

Rodriguez L, Simeonato E, Scimemi P, Anselmi F, Cali B, Crispino G, Ciubotaru CD, Bortolozzi M, Ramirez FG, Majumder P, et al. Reduced phosphatidylinositol 4,5-bisphosphate synthesis impairs inner ear Ca2+ signaling and high-frequency hearing acquisition. Proc Natl Acad Sci U S A. 2012; 109:14013–14018. [PubMed: 22891314]

Rohacs T, Thyagarajan B, Lukacs V. Phospholipase C mediated modulation of TRPV1 channels. Mol Neurobiol. 2008; 37:153–163. [PubMed: 18528787]

Rusinova R, Hobart EA, Koeppe RE 2nd, Andersen OS. Phosphoinositides alter lipid bilayer properties. J Gen Physiol. 2013; 141:673–690. [PubMed: 23712549]

Shields SD, Eckert WA 3rd, Basbaum AI. Spared nerve injury model of neuropathic pain in the mouse: a behavioral and anatomic analysis. J Pain. 2003; 4:465–470. [PubMed: 14622667]

Sorensen SD, Linseman DA, McEwen EL, Heacock AM, Fisher SK. A role for a wortmannin-sensitive phosphatidylinositol-4-kinase in the endocytosis of muscarinic cholinergic receptors. Mol Pharmacol. 1998; 53:827–836. [PubMed: 9584208]

Street SE, Walsh PL, Sowa NA, Taylor-Blake B, Guillot TS, Vihko P, Wightman RM, Zylka MJ. PAP and NT5E inhibit nociceptive neurotransmission by rapidly hydrolyzing nucleotides to adenosine. Mol Pain. 2011; 7:80. [PubMed: 22011440]

Tappe-Theodor A, Constantin CE, Tegeder I, Lechner SG, Langeslag M, Lepcynzsky P, Wirotanseng RI, Kurejova M, Agarwal N, Nagy G, et al. Galpha(q/11) signaling tonically modulates nociceptor function and contributes to activity-dependent sensitization. Pain. 2012; 153:184–196. [PubMed: 22071319]

Tong SE, Daniels SE, Black P, Chang S, Protter A, Desjardins PJ. Novel p38{alpha} Mitogen-Activated Protein Kinase Inhibitor Shows Analgesic Efficacy in Acute Postsurgical Dental Pain. J Clin Pharmacol. 2011; 52:717–728. [PubMed: 21659629]

Toth DJ, Toth JT, Gulyas G, Balla A, Balla T, Hunyady L, Varnai P. Acute depletion of plasma membrane phosphatidylinositol 4,5-bisphosphate impairs specific steps in endocytosis of the G-protein-coupled receptor. J Cell Sci. 2012; 125:2185– 2197. [PubMed: 22357943]

Unoki T, Matsuda S, Kakegawa W, Van NT, Kohda K, Suzuki A, Funakoshi Y, Hasegawa H, Yuzaki M, Kanaho Y. NMDA receptor-mediated PIP5K activation to produce PI(4,5)P(2) is essential for AMPA receptor endocytosis during LTD. Neuron. 2012; 73:135–148. [PubMed: 22243752]

van den Bout I, Divecha N. PIP5K-driven PtdIns(4,5)P2 synthesis: regulation and cellular functions. J Cell Sci. 2009; 122:3837–3850. [PubMed: 19889969]

Vasudevan L, Jeromin A, Volpicelli-Daley L, De Camilli P, Holowka D, Baird B. The beta- and gamma-isoforms of type I PIP5K regulate distinct stages of Ca2+ signaling in mast cells. J Cell Sci. 2009; 122:2567–2574. [PubMed: 19549683]

Volpicelli-Daley LA, Lucast L, Gong LW, Liu L, Sasaki J, Sasaki T, Abrams CS, Kanaho Y, De Camilli P. Phosphatidylinositol-4-phosphate 5- kinases and phosphatidylinositol 4,5-bisphosphate synthesis in the brain. J Biol Chem. 2010; 285:28708–28714. [PubMed: 20622009]

Wang Y, Lian L, Golden JA, Morrisey EE, Abrams CS. PIP5KI gamma is required for cardiovascular and neuronal development. Proc Natl Acad Sci U S A. 2007; 104:11748–11753. [PubMed: 17609388]

Wang YJ, Li WH, Wang J, Xu K, Dong P, Luo X, Yin HL. Critical role of PIP5KI{gamma}87 in InsP3-mediated Ca(2+) signaling. J Cell Biol. 2004; 167:1005– 1010. [PubMed: 15611330]

Weiss WA, Taylor SS, Shokat KM. Recognizing and exploiting differences between RNAi and small-molecule inhibitors. Nat Chem Biol. 2007; 3:739–744. [PubMed: 18007642]

Wenk MR, Pellegrini L, Klenchin VA, Di Paolo G, Chang S, Daniell L, Arioka M, Martin TF, De Camilli P. PIP kinase Igamma is the major PI(4,5)P(2) synthesizing enzyme at the synapse. Neuron. 2001; 32:79–88. [PubMed: 11604140]

White JK, Gerdin AK, Karp NA, Ryder E, Buljan M, Bussell JN, Salisbury J, Clare S, Ingham NJ, Podrini C, et al. Genome-wide generation and systematic phenotyping of knockout mice reveals new roles for many genes. Cell. 2013; 154:452–464. [PubMed: 23870131]

Xu W, Wang P, Petri B, Zhang Y, Tang W, Sun L, Kress H, Mann T, Shi Y, Kubes P, et al. Integrin-induced PIP5K1C kinase polarization regulates neutrophil polarization, directionality, and in vivo infiltration. Immunity. 2010; 33:340–350. [PubMed: 20850356]

Yu YL, Chou RH, Chen LT, Shyu WC, Hsieh SC, Wu CS, Zeng HJ, Yeh SP, Yang DM, Hung SC, et al. EZH2 regulates neuronal differentiation of mesenchymal stem cells through PIP5K1C-dependent calcium signaling. J Biol Chem. 2011; 286:9657–9667. [PubMed: 21216957]

Zylka MJ, Sowa NA, Taylor-Blake B, Twomey MA, Herrala A, Voikar V, Vihko P. Prostatic acid phosphatase is an ectonucleotidase and suppresses pain by generating adenosine. Neuron. 2008; 60:111–122. [PubMed: 18940592]

HIGHLIGHTS

1. PIP5K1C generates PIP_2 in somatosensory dorsal root ganglia neurons.
2. PIP5K1C regulates signaling through pronociceptive receptors.
3. Small molecule inhibitor of PIP5K1C identified.
4. Inhibition of PIP5K1C reduces sensitization in models of chronic pain.

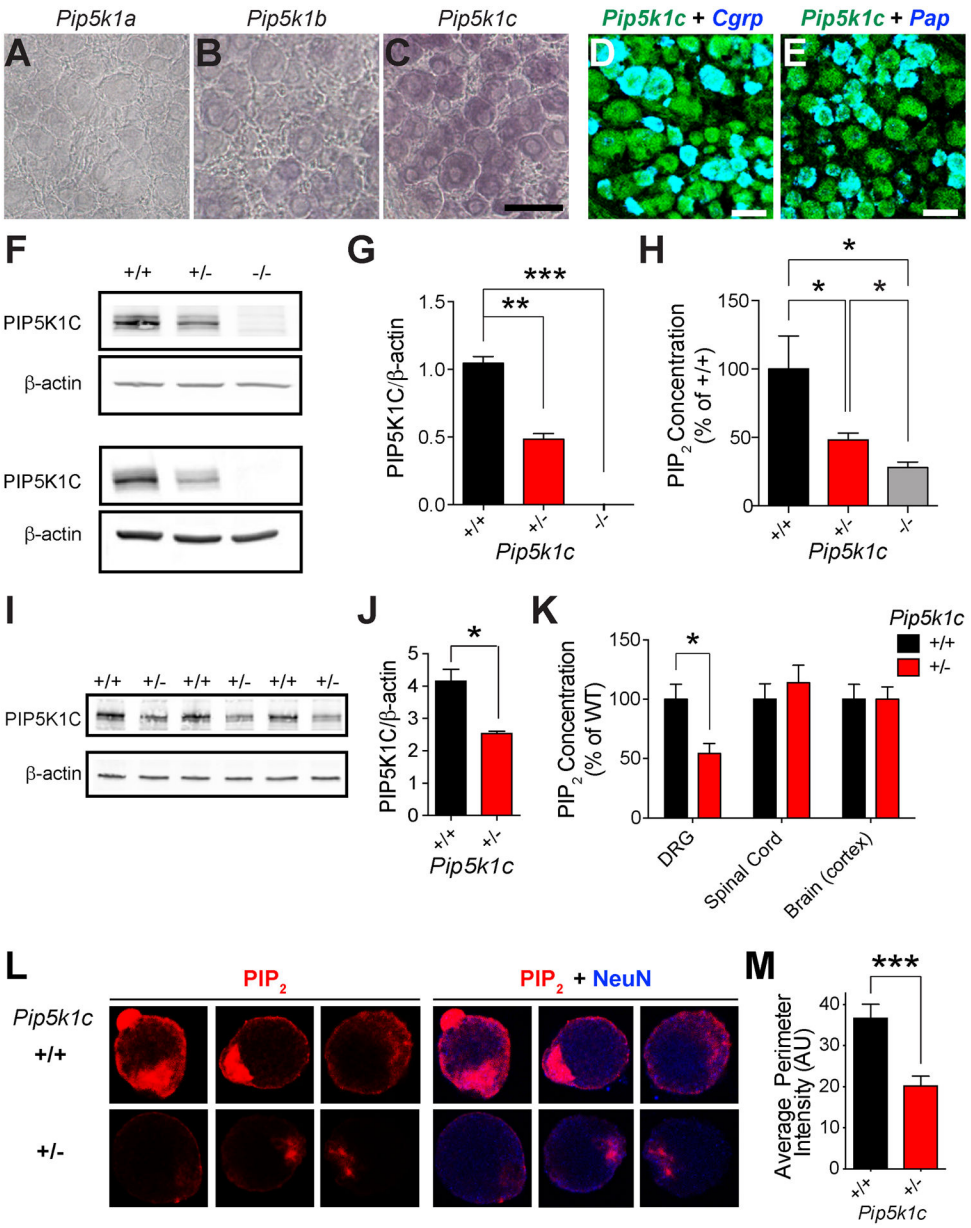

Figure 1. PIP5K1C is the predominant PIP_2 synthesizing enzyme in embryonic and adult DRG neurons

(A–C) *In situ* hybridization with gene-specific probes using sections from adult mouse lumbar DRG. Scale bar, 50 μm. **(D, E)** Double fluorescence *in situ* hybridization using adult lumbar DRG. Confocal images. Scale bar, 50 μm. **(F, G)** PIP5K1C protein levels in the DRG of WT, *Pip5k1c*$^{+/-}$, and *Pip5k1c*$^{-/-}$ embryonic (E17.5–18.5) mice relative to β-actin. **(F)** Representative western blots using two different antibodies (top (Di Paolo et al., 2004), bottom (Hara et al., 2013)) and **(G)** representative quantification for the Di Paolo et al. antibody; n=2–3 embryos per genotype. **(H)** PIP_2 levels in embryonic (E17.5–18.5) DRG quantified by a competitive binding enzyme-linked immunosorbent assay (ELISA) from WT, *Pip5k1c*$^{+/-}$, and *Pip5k1c*$^{-/-}$mice. n=10 embryos per genotype. **(I, J)** PIP5K1C protein

levels in adult DRG. **(I)** Western blots and **(J)** quantification; n=3 per genotype. **(K)** PIP_2 levels in DRG, spinal cord, and brain (cerebral cortex) of adult male *Pip5k1c*$^{+/+}$ and *Pip5k1c*$^{+/-}$ mice, quantified by ELISA. n=10 mice per genotype. **(L)** Representative images of membrane PIP_2 staining in small diameter DRG neurons cultured from *Pip5k1c*$^{+/+}$ and *Pip5k1c*$^{+/-}$ adult mice relative to NeuN and **(M)** quantification of the average perimeter (membrane) intensity. n=28 small diameter neurons quantified per genotype. All data are mean ± SEM. *p<0.05, ***p<0.0005. See also Figure S1.

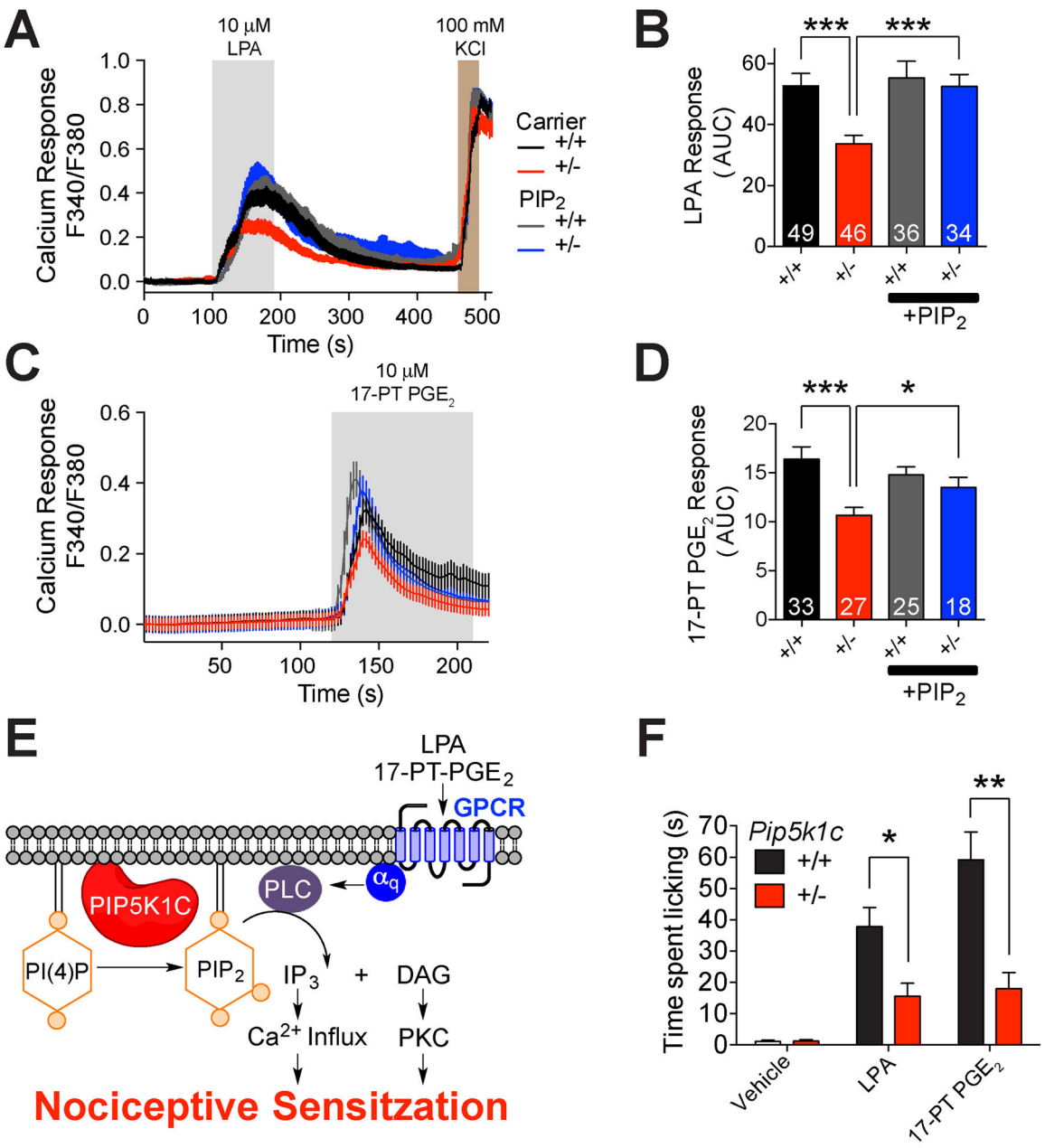

Figure 2. *Pip5k1c* haploinsufficiency reduces ligand-evoked nociceptive signaling *in vitro* and nocifensive licking *in vivo*

(A,C) Calcium responses and **(B,D)** quantification. Cultured adult DRG neurons were stimulated with **(A, B)** 10 μM LPA or **(C, D)** 10 μM 17-PT PGE_2 for 90 s, washed with HBSS for 120 s to remove the ligand, then stimulated for 30 s with 100 mM KCl to confirm neuron identity (not shown for 17-PT PGE_2). Cultures were incubated with 2 μM carrier or 2 μM Carrier + 2 μM PIP_2 for 15 minutes prior to calcium imaging. Number of neurons quantified is indicated in the bar graph. **(E)** Model. PIP5K1C generates PIP_2 that is hydrolyzed downstream of pronociceptive receptor activation. Ca^{2+} influx and PKC activation contribute to nociceptive sensitization. *Pip5k1c* haploinsufficiency reduces the

amount of PIP_2 that is available for signaling in DRG neurons. **(F)** Time spent licking for the first 5 minutes after injecting vehicle, 4.1 μg LPA, or 1.2 μg 17-PT PGE_2 into the left hindpaw of adult WT and *Pip5k1c*$^{+/-}$ male mice. n=10 per genotype per agonist. **(A–D, F)** All data are mean ± SEM. *p<0.05, ***p<0.0005. See also Figures S2, S3.

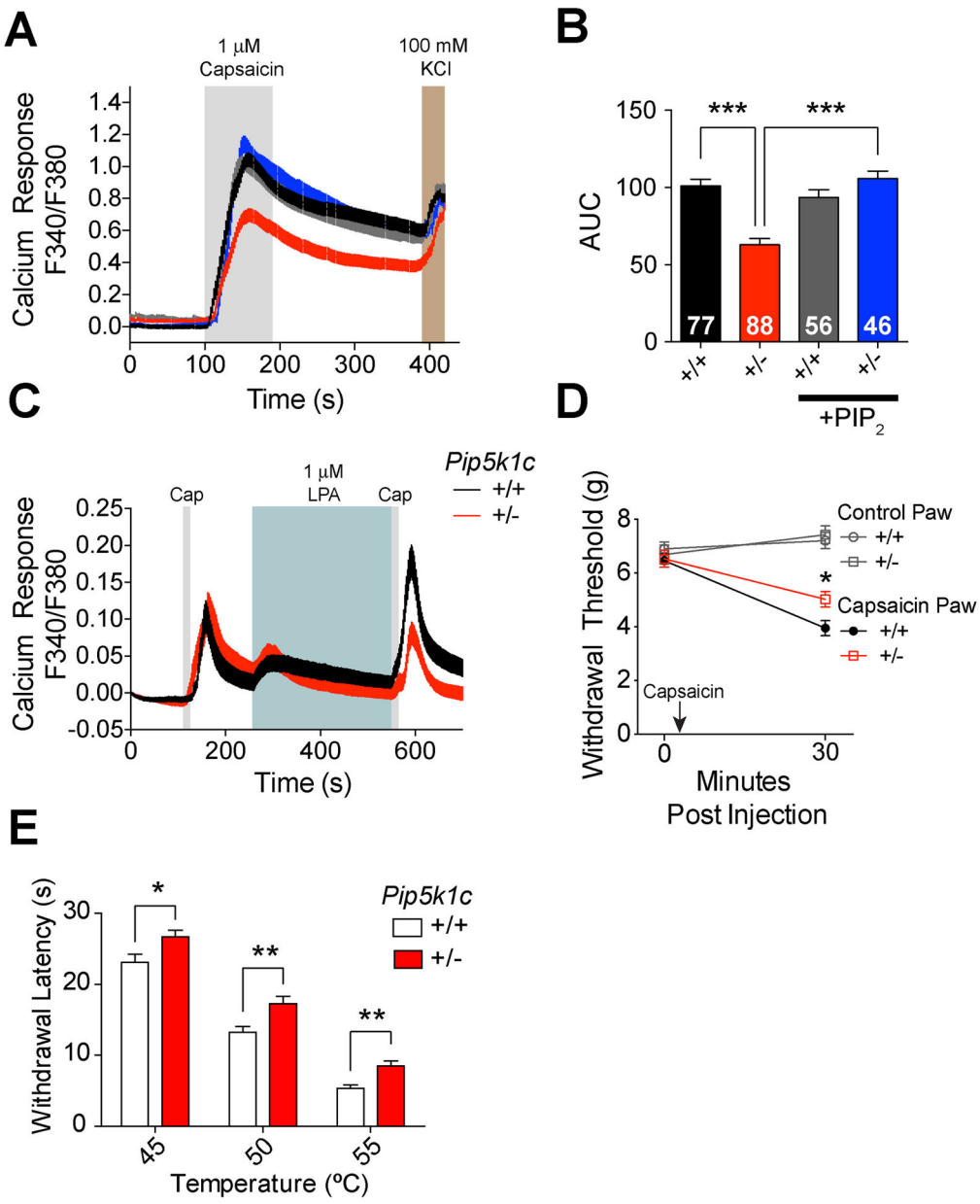

Figure 3. *Pip5k1c* haploinsufficiency reduces TRPV1-mediated nociceptive signaling *in vitro* and *in vivo*

(A) Capsaicin-evoked calcium responses and **(B)** quantification of cultured adult DRG neurons. Neurons were stimulated with 1 μM capsaicin for 90 s, washed with HBSS for 280 s, then stimulated for 30 s with 100 mM KCl to confirm neuron identity. Cultures were incubated with 2 μM carrier or 2 μM Carrier + 2 μM PIP_2 for 15 minutes prior to calcium imaging. Number of neurons quantified is indicated in the bar graph. **(C)** Capsaicin-evoked (Cap, grey, 100 nM) calcium responses before and after incubating with LPA. Average traces for 156 WT neurons and 143 *Pip5k1c*$^{+/-}$ neurons. **(D)** Mechanical sensitivity before and 30 minutes after intraplantar injection of 2 μg capsaicin. n=10 mice per genotype. **(E)**

Restrained hotplate assay. n=30 mice per genotype. All data are mean ± SEM. *p<0.05, **p<0.005, ***p<0.0005. See also Figure S3.

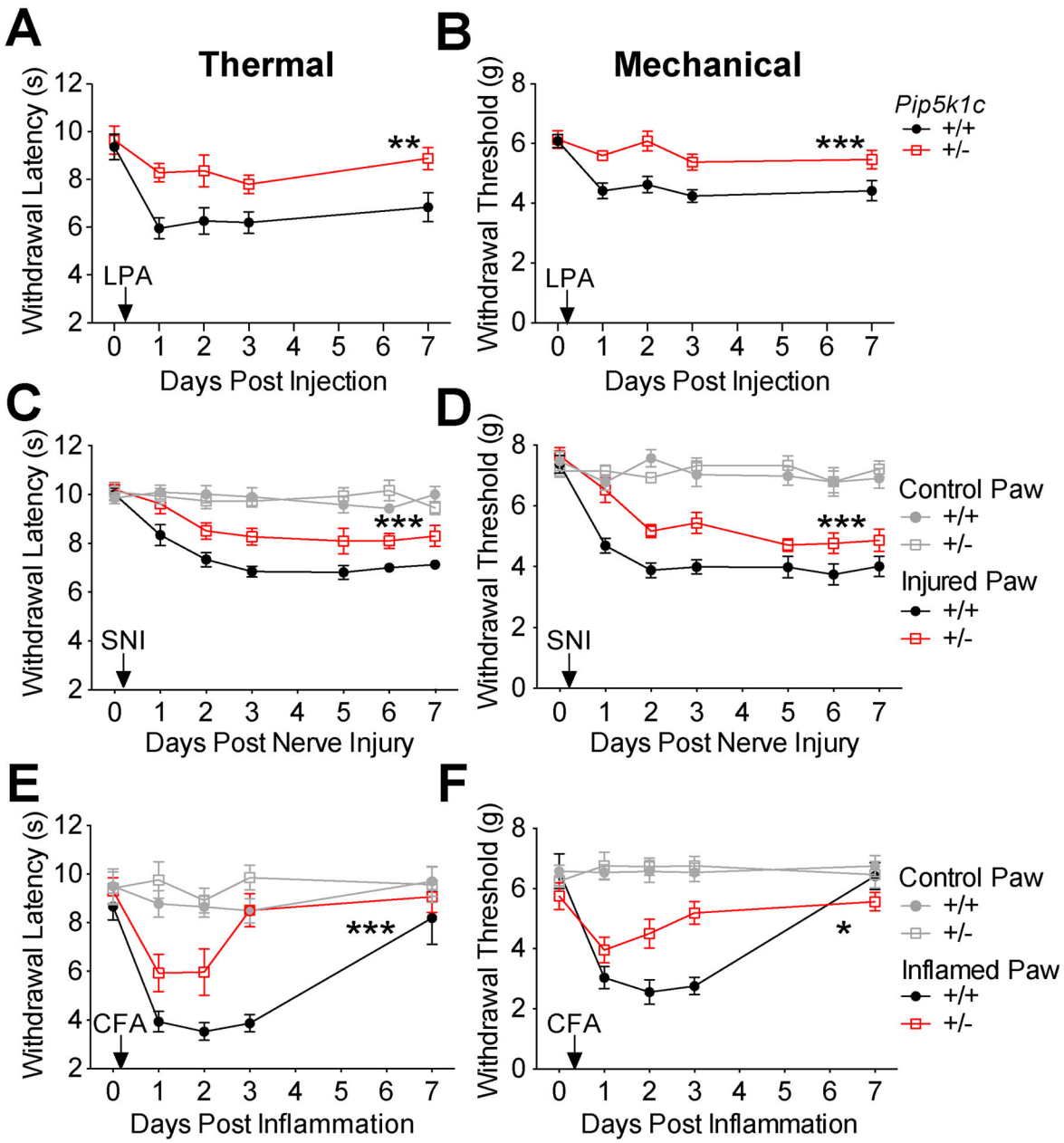

Figure 4. *Pip5k1c* haploinsufficiency attenuates thermal and mechanical sensitization in models of inflammatory pain and neuropathic pain

(A) Thermal (radiant heating; Hargreaves assay) and **(B)** mechanical (electronic von Frey) sensitivity in LPA-induced neuropathic pain model. LPA (1 nmol in 0.9% saline, i.t.) administered at the indicated time (arrow) to adult WT and *Pip5k1c*$^{+/-}$ mice. n=11 male mice per genotype. **(C)** Thermal and **(D)** mechanical sensitivity in the spared nerve injury model of neuropathic pain. Contralateral hindpaw served as a control. n=10 male mice per genotype. **(E)** Thermal and **(F)** mechanical sensitivity in CFA inflammatory pain model. CFA (20 μL) was injected into one hindpaw. Contralateral paw was not injected and served as a control. n=10 male mice per genotype. **(A–F)** All data are mean ± SEM. Asterisks

indicate significant difference between WT and *Pip5k1c*$^{+/-}$ mice by a one-way ANOVA. *p<0.05, **p<0.005, ***p<0.0005.

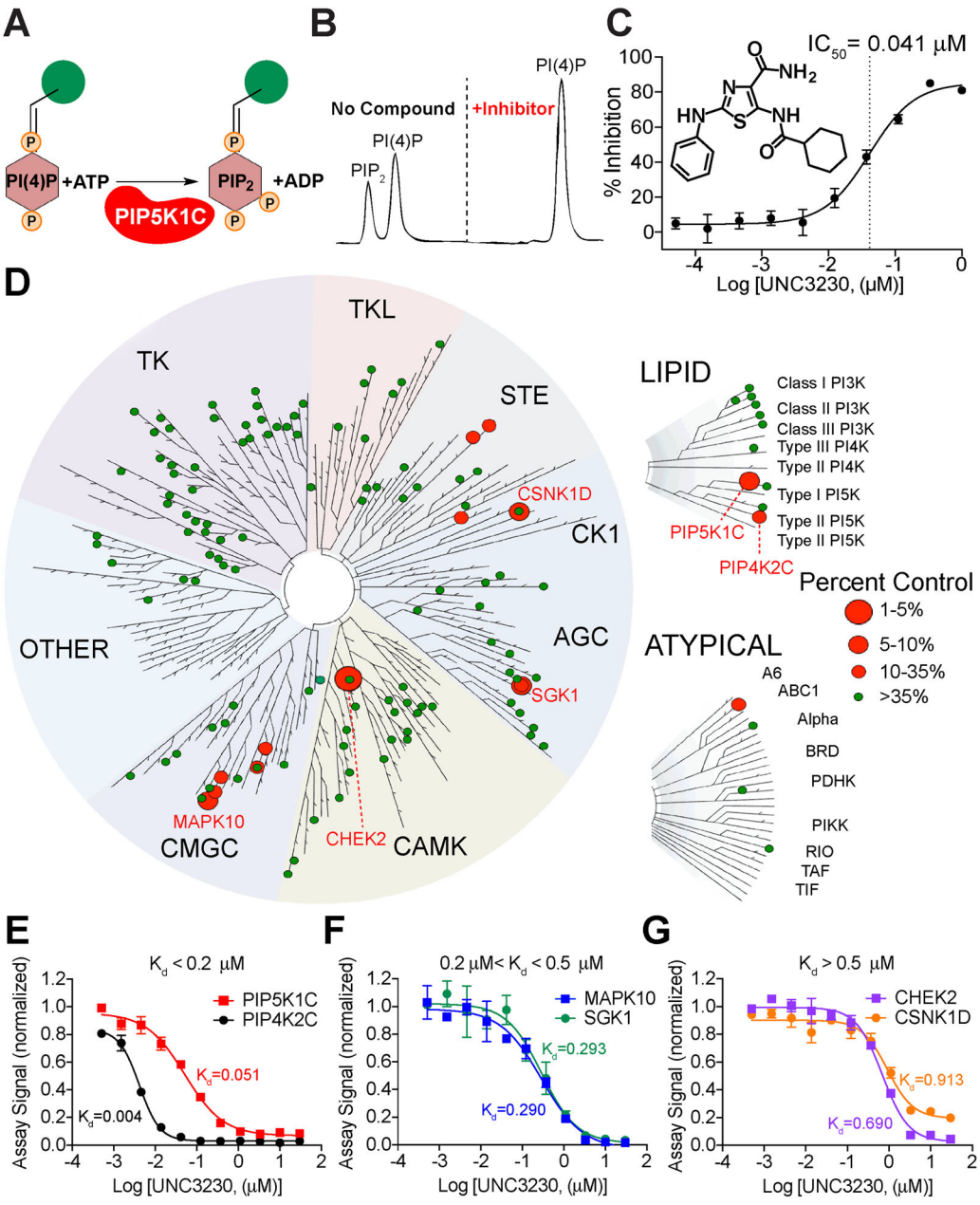

Figure 5. Identification of UNC3230 as a selective small molecule PIP5K1C inhibitor

(A) High-throughput screen is based on incubating fluorescein conjugated PI(4)P (substrate) with recombinant human PIP5K1C and then measuring product formation using a microfluidic mobility shift assay (LabChip). **(B)** Representative traces showing substrate and product peak separation in assay performed with and without a small molecule inhibitor (UNC3230; 10 μM). **(C)** UNC3230 structure and inhibitory concentration-50 (IC_{50}) doses-response curve, using LabChip assay. **(D)** Selectivity of UNC3230 relative to a diverse panel of kinases, using ProfilerPro (48 kinases) and KINOMEscan (100 kinases) assays. Table 1 lists all kinases that were tested. Circle size and color reflects percent activity/binding remaining in the presence of UNC3230 (10 μM) relative to controls. Branches without

circles denote kinases that were not tested. AGC: Containing PKA, PKG, PKC families; CAMK: Calcium/calmodulindependent protein kinase; CK1: Casein kinase 1; CMGC: Containing CDK, MAPK, GSK3, CLK families; STE: Homologs of yeast Sterile 7, Sterile 11, Sterile 20 kinases; TK: Tyrosine kinase; TKL: Tyrosine kinase-like. Image generated using TREEspot™ Software Tool and reprinted with permission from KINOMEscan®, a division of DiscoveRx Corporation, © DISCOVERX CORPORATION 2010. **(E–G)** KINOMEscan competitive binding assays with multiple doses of UNC3230, presented from **(E)** strongest K_d to **(G)** weakest K_d. All data are mean ± SEM. See also Figure S4.

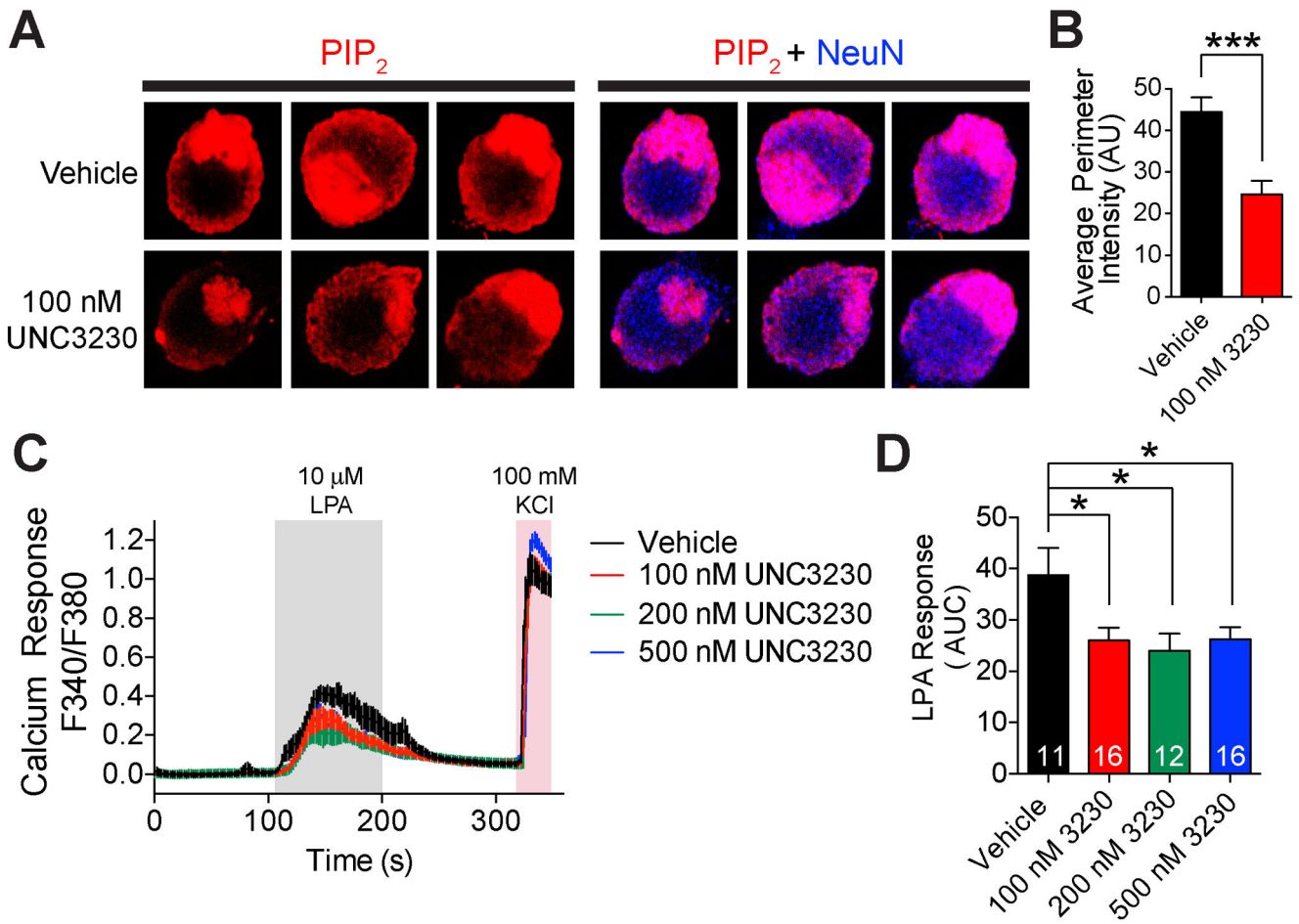

Figure 6. UNC3230 reduces membrane PIP_2 levels in DRG neurons and GPCR signaling

(A) PIP_2 antibody staining of WT DRG neurons after incubating with vehicle (0.002% DMSO) or 100 nM UNC3230 for 20 h. Co-stained with the neuronal marker NeuN (blue). **(B)** Quantification of the average perimeter (membrane) intensity. n=30–40 neurons per condition. **(C)** LPA-evoked calcium response in WT DRG neurons after incubating with vehicle or the indicated concentrations of UNC3230 for 20 h. After stimulation, cultures were washed with HBSS for 120 s to remove LPA, then stimulated for 30 s with 100 mM KCl to confirm neuron identity. **(D)** Quantification of the LPA-evoked calcium response by measuring the AUC of each responding neuron. Number of neurons quantified is indicated in bar graph. Data are mean ± SEM. *p<0.005, ***p<0.005.

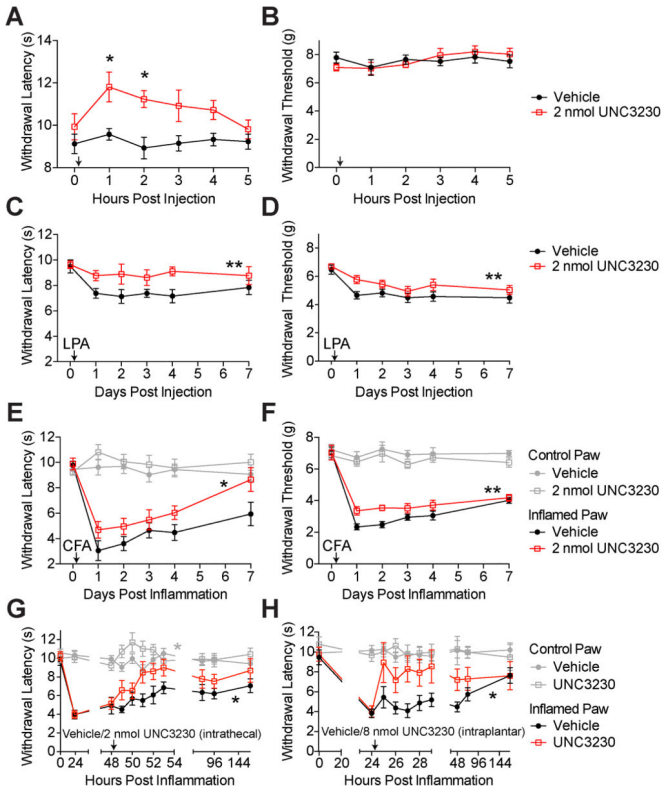

Figure 7. UNC3230 reduces thermal and mechanical sensitization in models of chronic pain

(A) Thermal and **(B)** mechanical sensitivity of WT mice after administering vehicle or 2 nmol UNC3230 (i.t.). Arrow indicates injection. n=10 male mice per group. **(C)** Thermal and **(D)** mechanical sensitivity of WT mice in the LPA-induced neuropathic pain model. Vehicle or 2 nmol UNC3230 were administered i.t. One hour later, vehicle or 2 nmol UNC3230 was administered i.t. with 1 nmol LPA. n=10 male mice per group. **(E)** Thermal and **(F)** mechanical sensitivity of WT mice in the CFA model of inflammatory pain. Vehicle or 2 nmol UNC3230 were administered i.t. Two hours later, CFA was injected into one hindpaw of each animal. The other hindpaw was not inflamed and served as a control. Vehicle or 2 nmol UNC3230 was administered (i.t.) 2 hours after CFA injection. n=10 male mice per group. **(G–H)** Thermal sensitivity of WT mice in the CFA model of inflammatory pain. CFA was injected into one hindpaw of each animal. The other hindpaw was not inflamed and served as a control. **(G)** Two days post CFA injection, vehicle or 2 nmol UNC3230 was administered i.t. n=10 male mice per group. **(H)** One day post CFA injection, vehicle or 8 nmol UNC3230 was administered into the inflamed hindpaw. n=10 mice per group. **(A)** One-way ANOVA with *post hoc* Bonferonni correction was used to compare differences between treatment groups for the 5 hour time course and at each hour. Black asterisks indicate significance at individual time points. ANOVA for the 5 hour time course, p=0.0045. **(C–H)** One-way ANOVAs were used to assess treatment effect over the 7-day time course (black asterisks). **(G)** One-way ANOVA was used to assess treatment effect in the non-inflamed paw over the 5 hour time course following injection (grey asterisk). All data are mean ± SEM. *p<0.05, **p<0.005. See also Figure S5.

Table 1

List of kinases screened for UNC3230 selectivity with numbers representing %activity/binding remaining in the presence of 10 μM UNC3230.

AGC	
AKT1	92*
AKT2	98*
CDC42BPA	98
DMPK	91
GRK1	96
P70S6K	74*
PDPK1	100
PRKACA	99*
PRKCB	109*
PRKCD	87
PRKCE	100
PRKCG	105*
PRKCZ	94*
ROCK2	99*
RPS6KA5	96*
RPS6KA3	85
RPS6KA1	85*
RPS6KB1	74*
SGK1	8, 23*
STK32C	80
ATYPICAL	
ADCK3	35
PDK2	93*
RIOK1	92
TRPM6	67
CAMK	
CAMK2A	98
CAMK2G	85*
CAMK4	93*
CHEK2	2.7
CHK1	101*
DCLK1	87
MAPKAPK2	85*
MAPKAPK5	89*
MARK1	89*

MARK3	100, 93*
MKNK1	95
MKNK2	46
MYLK3	46
NUAK2	100
PHKG1	60
PHKG2	88
PIM2	82*
PRKD1	84
STK11	100
TSSK1B	76
CK1	
CSNK1D	6.8, 54*
CSNK1G2	28
CMGK	
CDK16	94
CDK19	100
CDK2	93*
CDK3	100
CDK7	85
CDK9	99
DYRK1A	12
DYRK1B	16
GSK3B	88, 57*
MAPK1	109*
MAPK10	5.4
MAPK11	95
MAPK14	88, 130*
MAPK3	91*
MAPK8	32
MAPK9	15
SRPK3	100
LIPID	
PI4KB	67
PIK3C2B	78
PIK3C2G	93
PIK3CA	77
PIK3CB	95
PIK3CD	90
PIK3CG	82
PIP4K2B	100
PIP4K2C	14

PIP5K1A	100
PIP5K1C	7
OTHER	
AAK1	47
AURKA	76*
AURKB	91
CHUK	82
IKBKB	100
PLK1	73
ULK2	79
STE	
MAP2K1	89
MAP2K2	82
MAP3K4	93
MAP4K4	28, 27*
MINK1	35
MYO3A	64
MYO3B	49
PAK1	92
PAK2	99*
PAK4	60
STK3	100*
TK	
ABL	92*
ALK	54
AXL	75
BTK	102*
CSF1R	100
EGFR	98
EPHA2	100
ERBB2	97
FGFR1	96*
FGFR2	100
FLT3	90*
FYN	88*
INSR	100*
ITK	94
JAK2	70
JAK3	94
KDR	100*
KIT	100

LCK	93*
LYN	97*
MET	75*
MUSK	100
NTRK1	99
NTRK2	83
NTRK3	89
PDGFRA	81
PDGFRB	100
PTK2	97
PTK2B	99
RET	100
SRC	95*
SRMS	81
SYK	93*
TEC	89
TIE1	91
TYK2	86
TYRO3	94
ZAP70	89
TLK	
ACVR1B	89
BMPR2	80
BRAF	94
IRAK4	93*
LIMK1	100
MAP3K9	74
RAF1	91*
TGFBR1	96

*Screened using the PerkinElmer ProfilerPro assay, all others screened using the DiscoveRx KINOMEscan assay.